

UPCommons

Portal del coneixement obert de la UPC

<http://upcommons.upc.edu/e-prints>

Aquesta és una còpia de la versió *author's final draft* d'un article publicat a la revista *Engineering structures*.

URL d'aquest document a UPCommons E-prints:

<https://upcommons.upc.edu/handle/2117/134171>

Article publicat / *Published paper*:

Bernat, E.; Gil, L. Assessing the performance of CFRP strengthening on masonry walls using experimental modal analysis. "Engineering structures", 15 Agost 2019, vol. 193, p. 184-193.

Assessing the performance of CFRP strengthening on masonry walls using experimental modal analysis

Ernest Bernat-Masó^{a*}, Lluís Gil^b

^a Serra Húnter Fellow. Strength of Materials and Structural Engineering Department, Universitat Politècnica de Catalunya. C/ Colom 11, TR45. 08222 Terrassa

^b Strength of Materials and Structural Engineering Department, Universitat Politècnica de Catalunya. C/ Colom 11, TR45. 08222 Terrassa

* Corresponding author. ernest.bernat@upc.edu

Abstract

Strengthening masonry structures using FRP laminates has been widely studied from a resistance point of view. However, there is a need of a non-destructive technique to validate strengthening interventions. In this paper, experimental modal analysis is proposed as a technique to assess practitioners' works. Fifteen brick masonry walls were built and strengthened with five different patterns of carbon-FRP laminates. Experimental modal analysis was performed before and after strengthening interventions. Different vibration modes were compared to select the more sensitive one depending on the strengthening configuration. The change in the vibration frequency was analysed and correlated with cross-section stiffness modification. The obtained results showed changes up to 30% on the vibration frequencies due to strengthening installation. On the overall, the proposed experimental methodology is supported by theoretical analytical calculations with an error under 5% in most of the cases.

Keywords

Experimental Modal Analysis, Masonry walls, Fibre Reinforced Polymers, Strengthening assessment, Analytical frequency calculation.

1. Introduction

Strengthening masonry structures with externally bonded FRP is a consolidated technique that has focused the research of several authors in the last years. Effectiveness of FRP has been analysed for different masonry structures (pillars [1,2], walls [3,4] or vaults [5,6]), different types of FRP and different loading conditions: compression [7], static shear [8], cyclic shear [9], static bending [10] or cyclic bending [11].

Mechanical performance of FRP is out of doubt, reaching load-bearing capacity increments over 70% for pillars thanks to FRP confinement [12], around 100% in bending thanks to tensile contribution of FRP [13], over 22% against shear efforts [14] and over 100 times in the case of arches [15].

Nevertheless, moisture sensitivity of FRP may cause inappropriate connection between masonry substrate and FRP strengthening system [16]. Thus, although FRP strengthening system uses industrialised materials (laminates, epoxy resins), its manual application may result into structural problems associated with adhesive voids or improper curing. In this context, it is important to implement strict control procedures and visual inspection campaigns (see [17]). However, developing a reliable tool to assess the mechanical response of strengthened structures can ease those inspection tasks.

One possible option is to perform service load tests in a way that a controlled load is applied on the structure and the deformation result is measured. This kind of tests bring an idea of the stiffness variation of a structure if comparing before-strengthening and after-strengthening stages. However, this approach is space-invasive and expensive. Only laboratory tests can be found with this approach that is no common in real practice. On the other hand, detailed inspection of FRP-masonry interface can be performed using ultrasound or georadar techniques

[18]. However, this type of local inspection is expensive and does not bring an idea of the global effect of the strengthening on the structure.

Finally, some authors proposed using modal analysis to assess the performance of FRP-strengthening because vibrational parameters highly depend on structure stiffness, which is expected to be highly affected if a high-stiffness material, like FRP, is bonded to the existing structure.

Researches using modal analysis have been performed to characterise masonry or concrete structures. Most of them (for example [19,20]) were based on operational modal analysis, so structure was indirectly excited by environment and global vibration parameters, like main vibration frequencies, can be determined. In contraposition, other authors proposed using experimental modal analysis, which crosses load and acceleration data to obtain modal shapes, associated frequencies and damping values. Some applications of this technique were conducted on different structures from concrete beams [21] to rammed earth walls [22]. All concluded that modal analysis is a high-potential non-destructive technique for the structural assessment of large structures. Among them, a few authors used experimental modal analysis to detect vibrational changes due to strengthening operations. Corradi et al. [23] used this technique to evaluate the effect of damaging a masonry vault and repairing it with FRP strips. In the same line, Cakir et al. [24] studied the influence of cracking and FRP-strengthening reinforced concrete beams. Thus, experimental modal analysis has been used as a comparative tool for assessing the performance of FRP strengthening in particular cases. However, the dependency of the vibrational response on the strengthening patterns or the setting criteria for the elections of the suitable vibration modes to be analysed has not been conducted yet as per authors' knowledge.

Looking at the overall context it seems that FRP system is a well-established strengthening technique for masonry structures although there are no deeply studied procedures based on experimental modal analysis to assess the mechanical performance of the structure after FRP installation. Many data will be required to calibrate and validate this particular application. In this line, the changes on vibrational parameters of out-of-plane excited solid clay brick masonry walls due to FRP-laminate strengthening system, installed according five different patterns, are studied to conclude about the more sensitive parameters for analysis, the relationship between the strengthening pattern and the modified modal shapes and the range of variation of vibration frequency. Finally, analytical predictions of the vibration frequencies of strengthened walls are compared with experimental results showing good accuracy, which supports the reliability of the proposed methodology.

2. Experimental campaign

2.1. Materials and methods

2.1.1. Wall specimens

Fifteen brickwork wall specimens were built for the discussion of the performance of modal analysis to assess the FRP-strengthening intervention. These walls are described in detail in [4], where their mechanical response under axially eccentric compressive load is analysed.

Solid fired clay bricks (265mm x 125mm x 50mm, with tensile strength $f_{tb} = 2.8\text{MPa}$ and compressive strength $f_{cb} = 27.9\text{MPa}$, see [25]) and general-purpose M7.5 Portland cement mortar (compressive strength $f_{cm} = 3.7\text{MPa}$ and flexural strength $f_{xm} = 1.25\text{MPa}$, see [25]) were used to build the walls. Carbon FRP laminate strips (1.2mm x 80mm section, tensile strength of 3100MPa and elastic modulus of 170GPa, see [4]) were installed using epoxy resin additive after preparing the substrate with a primer epoxy resin. General geometric properties (height, H , width, b and

thickness, t) and strengthening configurations (number of vertical, horizontal and inclined laminates in the 6th-8th columns respectively) are summarised in Table 1. The number and orientation of strengthening laminates defines the labelling of the walls. Figure 1 represents the strengthening patterns. For 2V0H and 3V0H walls, the strengthening pattern was the same then for 2V2H and 3V5H respectively but without the horizontal strips. Only one face of each wall was strengthened.

<i>Series</i>	<i>Wall</i>	<i>H (mm)</i>	<i>t (mm)</i>	<i>b (mm)</i>	<i>#_{v,FRP}</i>	<i>#_{h,FRP}</i>	<i>#_{i,FRP}</i>	<i>α (°)</i>	<i>d_v (mm)</i>	<i>d_h (mm)</i>
2V0H	1	1587	126.5	837					126	199
	2	1609	125.9	840	2	0	0	---	128	199
	3	1591	126.1	838					126	200
3V0H	1	1602	126.4	829					127	196
	2	1602	126.3	833	3	0	0	---	127	198
	3	1612	126.3	837					128	198
2V2H	1	1579	126.1	843					125	199
	2	1589	124.4	835	2	2	0	---	127	199
	3	1592	124.7	827					126	196
3V5H	1	1575	123.8	833					130	198
	2	1580	124.7	830	3	5	0	---	131	197
	3	1552	124.5	831					128	197
3I3I	1	1625	124.3	826					129	196
	2	1622	124.6	831	0	0	3+3	61	129	198
	3	1608	123.8	827					128	198

Table 1. Geometry and strengthening definition. Values of 4th-9th columns are edited from data in [4].

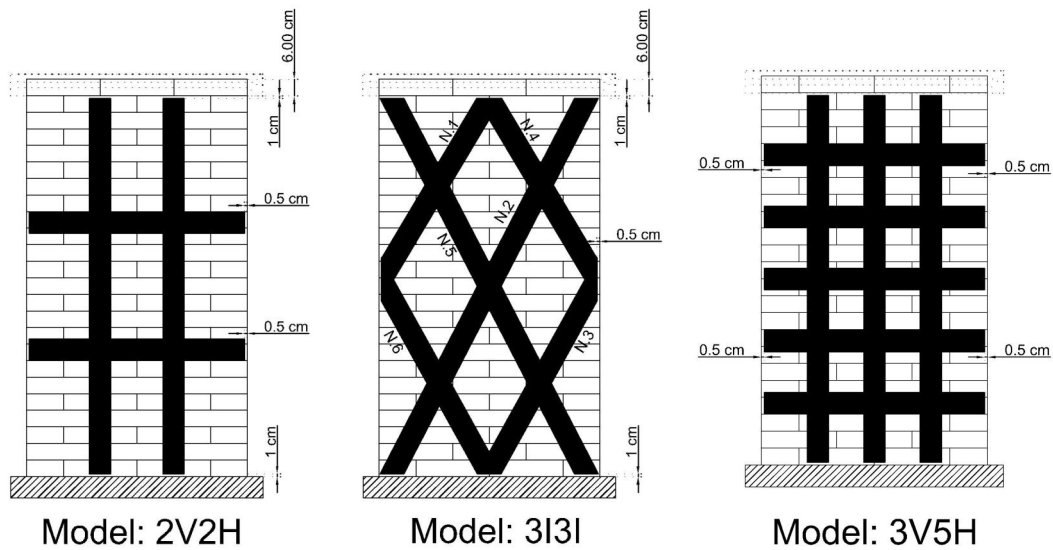


Figure 1. FRP strengthening patterns

2.1.2. Experimental modal analysis

Experimental modal analysis fits into the category of input-output experimental modal identification tests, in which different points are excited and the vibration response (in terms of acceleration) is measured in a fixed point. In particular, the proposed experimental campaign had the aim of capturing the out-of-plane vibration modes (shape, frequency and damping) and analysing how strengthening patterns affected them.

To perform it, the procedure described in [22] was implemented. Two modal analyses were undertaken for each wall: one before strengthening and the other one after curing the strengthening system. In order to carry out experimental modal analysis, 55 points were defined on the non-strengthened face of each wall forming a grid of 11 rows and 5 columns. Points spacing depended on wall geometry and these are summarised in 10th and 11th columns of Table 1.

A unidirectional accelerometer (Brüel&Kjær piezoelectric charge accelerometer type 4370 with charge converter type 2646, sensitivity of 10.11pC/ms⁻² and measuring range up to 4.8kHz) was placed in the top left point of the drawn grid because of the presumed high displacement

amplitude and contribution of the displacement of this point in each vibration mode. In other words, installing the accelerometer in the top left position avoided the possibility of placing it in a zero displacement point for the particular structural configuration that was experimentally analysed. This sensor was oriented along the transversal direction (out-of-plane direction). Regarding the fixation procedure, accelerometer was attached to a transmission plate, which was bonded to the wall using cyanoacrylate, like in previous experiences, [22]. Placing additional accelerometers would have been preferable to make data more independent of the only-one accelerometer installation point. However, acquisition limitations and the expectation of using as simple as possible configuration test drove to the made choice which proved to be effective at a lower cost for simple structures as presented later on. In the case of extending the herein described method to different boundary conditions or analysing a wall which is part of a complex building, it would be recommended to place the accelerometer at a position which was generally associated to large displacements in the firsts theoretical vibration modal shapes, which may be obtained with simple numerical simulations on elastic hypothesis.

An impact hammer (Brüel&Kjær type 8206 with rubber tip) was used to excite the wall by impacting on all points in the out-of-plane direction.

Brüel&Kjær Multipurpose 6-channel input module type 3050-B-060 was used to acquire the data. A transient time weighting was defined to select the significant impact data from the hammer. An exponential time weighting was defined to select the significant oscillation data from the accelerometer, discarding the data of the oscillation forced by the own impact process. A domain span of 500Hz was defined and the precision of frequency was set to 0.31Hz.

Using PULSE™ software, impact hammer and accelerometer data were independently acquired in the time domain considering the respective windowing functions explained before. After

selecting the data to process for each signal, these were automatically subjected to a Fast Fourier Transformation by the analyser. It also calculated the auto-spectrum of each signal and the cross-spectrum of the signals to finally obtain the Frequency Response Function (FRF) associated with the impact. The FRF calculation removes the force spectrum from the data resulting in only the inherent information that describes the structural response between the impact point and the accelerometer reading point. This procedure was repeated for a second hammer impact on the same point. Then, the coherence within the two impacts was calculated. If coherence was acceptable (coherence values close to 1 except for the points close to resonance frequencies) the average of the FRFs of the two impact repetitions on the same point was calculated and stored. This procedure was repeated for all impact points.

Using MESocpeVES™ software, the peaks of the Frequency Response Spectrum (set of averaged FRFs associated with all impact points) were counted considering the imaginary part of the signal only (see Figure 2). After that, a global curve fitting on the functions was defined using Single Degree Of Freedom CoQuad plot (real and imaginary part vs. frequency) method, which forced the calculated vibration modes to have only a real part, making the comparison with numerical simulation or analytical approaches easier. The residues of the curve fitting were calculated. Finally, modal shapes, their corresponding frequencies and damping values were obtained. Two examples of FRFs can be observed in Figure 3, where the effect (changing frequency they are located) of the strengthening intervention on the peaks of the FRFs is evident for wall 3V5H_2. More details on experimental input-output modal analysis data process are described in [26].

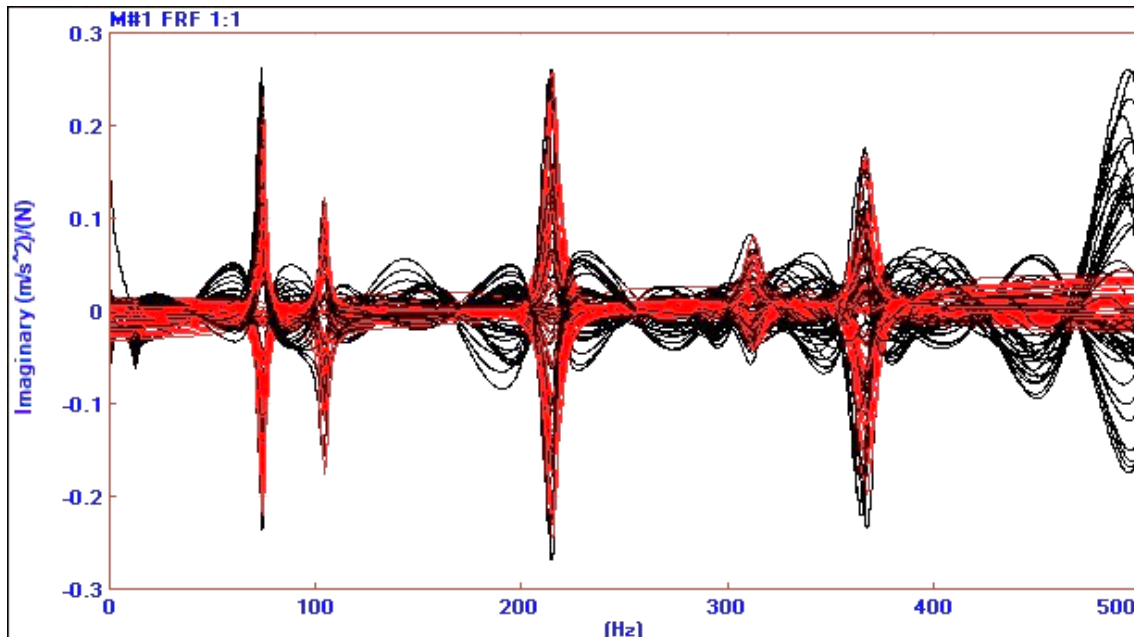
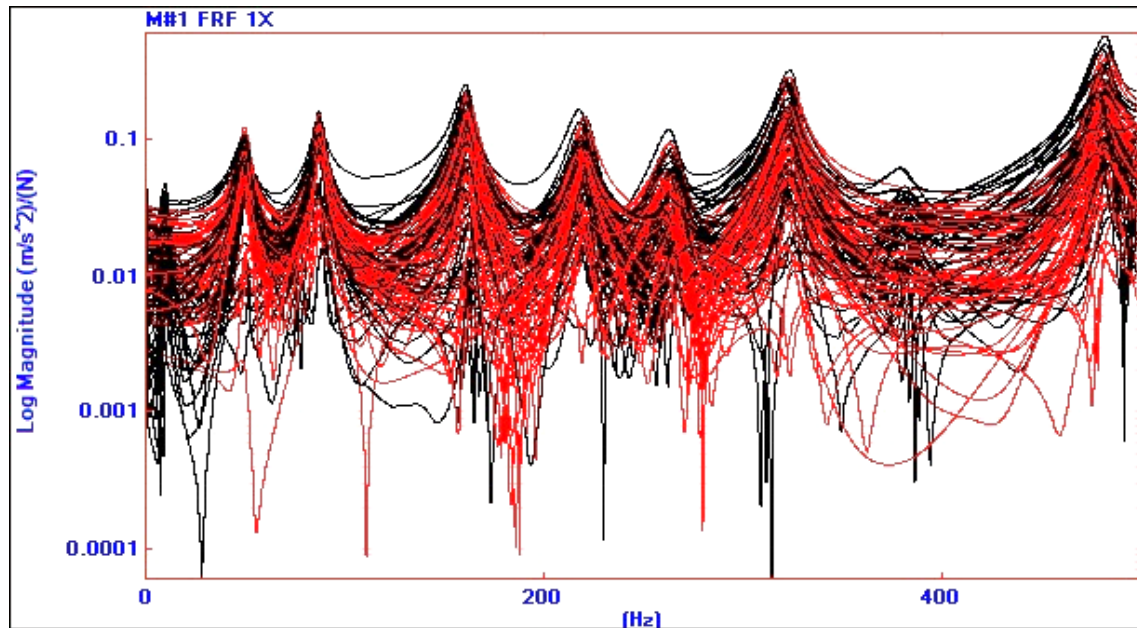


Figure 2. Imaginary part of the FRFs (black) and the corresponding fitted curves (red) for strengthened wall 2V0H_3

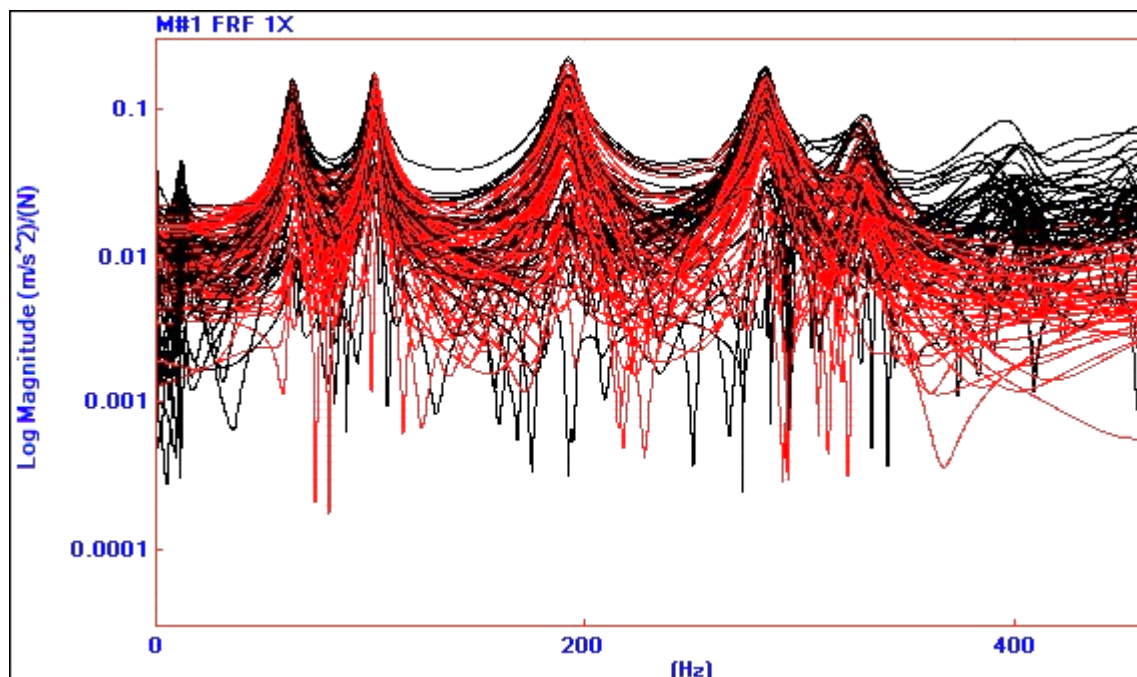
During the modal testing, silent environmental conditions with low externally-induced vibrations due to traffic or other laboratory activities were guaranteed planning the time of test execution. Walls were physically supported standing on their basis during modal testing with no additional constrains.

After performing the first modal testing campaign, walls were strengthened as explained with detail in [4]: cleaning surface, applying a primer layer and leaving it dry for 24h, cutting CFRP laminate strips, bonding CFRP strips to the wall surface using bi-component epoxy adhesive and repeating the adhesion operation of the over-crossing strips in the cases 2V2H, 3V5H and 3I3I.

After 7 days of adhesive curing at indoor environmental conditions (22°C, RH60%), modal analysis was repeated with exactly the same structural configuration and same laboratory conditions so to obtain comparable results. Walls were not moved between first and second modal analysis and the grid used to define the impact points was also maintained.



No strengthened



Strengthened

Figure 3. FRFs (black) and the corresponding fitted curves (red) for unstrengthened (top) and strengthened (bottom) wall 3V5H_2

2.2. Experimental results

A maximum of five vibration modes have been analysed although all of them were not observed in all experimental tests after data post-processing. The observed vibration modes (shapes and corresponding labelling) and the values of the corresponding frequencies (ω_u for unreinforced walls and ω_s for CFRP-strengthened walls) and damping ratios (ζ_u for unreinforced walls and ζ_s for CFRP-strengthened walls) are summarised in Table 2 for unstrengthened cases and in Table 3 for the same walls after strengthening.

		Vibration mode									
		Mode 1		Mode 2		Mode 3		Mode 4		Mode 5	
<i>Wall</i>		ω_u (Hz)	ζ_u (%)	ω_u (Hz)	ζ_u (%)	ω_u (Hz)	ζ_u (%)	ω_u (Hz)	ζ_u (%)	ω_u (Hz)	ζ_u (%)
2V0H	1	77.20	2.70	88.09	2.67	236.96	1.41	---	---	395.20	1.45
	2	69.82	2.76	78.97	2.54	223.69	1.30	332.21	1.15	370.42	1.54
	3	51.11	6.66	90.00	2.40	165.97	2.50	---	---	317.87	1.16
3V0H	1	77.06	2.54	81.74	2.48	243.98	1.19	369.15	1.40	410.42	1.09
	2	76.07	2.58	87.19	2.53	262.36	1.53	---	---	---	---
	3	71.06	2.90	86.59	2.52	229.38	2.06	---	---	388.55	2.35
2V2H	1	74.69	2.69	84.84	2.48	232.29	1.45	352.83	1.22	391.64	1.36
	2	70.08	2.99	---	---	---	---	311.75	1.75	368.44	0.82
	3	36.30	2.76	---	---	222.62	1.56	312.18	1.65	356.92	1.78
3V5H	1	27.71	7.24	81.10	2.60	143.49	1.84	337.42	1.00	303.97	0.86
	2	50.20	5.03	87.70	2.46	162.09	2.05	---	---	264.60	2.04
	3	72.08	2.81	84.34	2.58	217.88	1.68	---	---	---	---
3I3I	1	71.68	2.75	77.57	2.64	223.14	1.64	339.28	1.66	388.97	1.67
	2	72.88	2.64	78.28	2.50	225.49	1.25	---	---	385.73	1.24
	3	68.47	2.83	---	---	224.13	1.32	---	---	379.55	1.35
CoV		24.1	44.6	5.0	3.1	15.7	22.9	6.1	20.7	11.7	30.7

Table 2. Vibration modes, frequencies and damping ratios for unstrengthened brick masonry walls

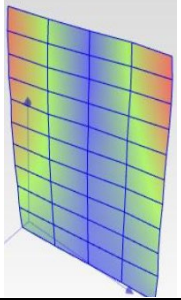
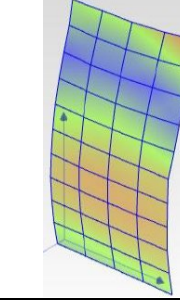
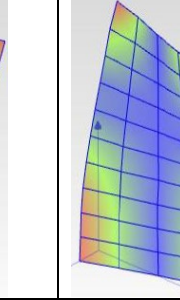
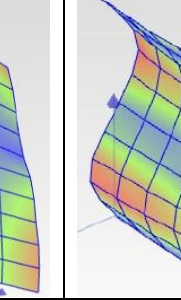
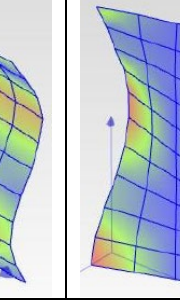
		<i>Vibration mode</i>									
											
		Mode 1		Mode 2		Mode 3		Mode 4		Mode 5	
<i>Wall</i>		ω_s (Hz)	ζ_s (%)	ω_s (Hz)	ζ_s (%)	ω_s (Hz)	ζ_s (%)	ω_s (Hz)	ζ_s (%)	ω_s (Hz)	ζ_s (%)
2V0H	1	80.24	2.40	97.60	3.03	241.05	1.48	--	--	406.93	1.38
	2	72.68	2.66	85.07	2.42	231.16	1.21	355.21	1.05	386.22	1.24
	3	74.54	3.07	104.77	2.12	215.72	1.96	---	---	368.23	1.57
3V0H	1	79.94	2.37	90.04	2.27	252.73	1.22	394.58	1.29	427.09	1.28
	2	85.83	2.36	104.64	2.23	---	---	---	---	---	---
	3	73.79	2.71	95.53	2.33	236.03	1.43	---	---	407.61	2.19
2V2H	1	76.93	2.66	89.46	2.66	239.40	1.61	378.36	1.23	---	---
	2	72.23	2.97	---	---	---	---	337.90	1.62	386.63	1.80
	3	74.17	2.78	81.55	2.46	237.36	1.60	354.00	1.42	385.35	1.75
3V5H	1	77.59	2.71	102.07	2.18	235.20	1.47	---	---	405.32	1.18
	2	64.10	4.16	102.70	2.23	192.76	2.35	---	---	330.29	2.01
	3	86.66	2.45	103.86	2.09	260.76	1.30	---	---	---	---
3I3I	1	90.25	2.88	103.56	2.31	274.41	1.24	---	---	---	---
	2	88.72	3.42	99.95	2.05	272.83	1.25	---	---	491.97	1.01
	3	79.91	2.57	243.26	1.81	266.91	1.51	---	---	460.74	1.30

Table 3. Vibration modes, frequencies and damping ratios for brick masonry walls after strengthening

3. Analytical approach

3.1. Method

The structural configuration of the walls was modelled as a cantilever beam. Real support (walls standing on their base) was not a pure simply-supported boundary condition neither a pure fixed support. In addition, the great stabilising effect of self-weight and the little magnitude of the applied excitation justified the decision of modelling walls as fixed at the bottom side. This hypothesis was more representative than the alternative of allowing free out-of-plane rotation in

the bottom support that never happened during tests. Hence, cantilever beam approach was used in the following analytical calculations although it was in conflict with some mode shapes (mode 3 and mode 5) which cannot either be analysed with the proposed analytical unidimensional simplification. This conflict was not really relevant for the next steps as long as the analytical approach was based on the out-of-plane bending modes (mode 2 and mode 4) which experimentally met the assumed bottom-fixed constrain. The selection of the bending modes for the analysis is justified later on and it is based on the major influence that the strengthening intervention had on these vibration modes.

Notice that the excitation of the structure during experimental modal analysis produce a dynamic response that relies inside the elastic constitutive behaviour of the masonry. Hence, there is no crack or non-linear effects and the relationship between bending stiffness (EI) and free bending vibration frequencies (ω) of a cantilever beam can be adapted to unstrengthened walls (Eq. 1) and CFRP-strengthened walls (Eq. 2) as follows:

$$\omega_u(\text{Hz}) = \frac{\alpha_n^2}{2\pi} \sqrt{\frac{E_m I_u}{\rho b t H^4}} \quad (\text{Eq. 1})$$

$$\omega_s(\text{Hz}) = \frac{\alpha_n^2}{2\pi} \sqrt{\frac{E_m I_s}{\rho b t H^4}} \quad (\text{Eq. 2})$$

Where $\alpha_n = 4.694$ for vibration mode 2 and $\alpha_n = 7.855$ for vibration mode 4. It has to be noticed that the first theoretical cantilever vibration mode ($\alpha_n = 1.875$) was neglected from the analysis because it was not experimentally observed. It may be justified because the acquired response was not accurate enough for low frequencies in order to distinguish the first theoretical bending mode from the superposed solid rigid movements. In addition, the real wall support was not totally fixed (but close to a fixed one) and it may justify that the first expected bending mode of a

cantilever beam was not properly captured by the performed modal analysis. Finally, the good accuracy of the second and third theoretical bending modes of a cantilever beam with the corresponding experimental vibrational data (mode 2 and mode 4 respectively) supports the modelling it as a cantilever beam.

Mode 2 and mode 4, which are graphically defined in Table 2, were selected because of the significant variation of their vibration frequency due to CFRP installation, as it can be observed in experimental results (see Table 2 and Table 3). ρ is the density of the material the wall (cantilever beam) is made of, bt is the area of its transversal cross-section and H is the height of the wall (length of the beam). E_m is the effective dynamic elastic modulus of masonry and I_u ($I_u=1/12 \cdot b \cdot t^3$) and I_s are the modulus of inertia of the cross-section of unstrengthened walls and CFRP-strengthened walls respectively.

The effective dynamic stiffness ($E_m I_u$) of every unstrengthened wall was calculated from the corresponding experimental vibration frequency (ω_u in Table 2) for both bending modal shapes (mode 2 and mode 4) using equation (Eq. 1). Therefore, the effective dynamic stiffness ($E_m I_u$) of each unstrengthened wall (see Table 4 and Table 5) and the corresponding elastic modulus of masonry, E_m , were calculated from purely experimental data.

The installation of CFRP strips modified the stiffness of the wall. Using a homogenised equivalent section, within elastic theory, a new mechanical effective dynamic stiffness, $E_m I_s$, was analytically calculated for each wall with the common procedure for composite sections:

- a) defining the ratio between the elastic modulus of CFRP (E_{FRP}) and the masonry effective dynamic elastic modulus (E_m);
- b) defining the equivalent width of a masonry part equivalent to the corresponding FRP section.

c) calculating the bending modulus of inertia of the homogenised strengthened section (I_s) composed of the initial masonry section and the masonry part equivalent to the corresponding FRP section.

d) calculating the equivalent mechanical effective dynamic stiffness, $E_m I_s$ using the previous analytical result (I_s) and the corresponding masonry effective dynamic elastic modulus (E_m), which was experimentally determined for each particular case.

The initial CFRP section of inclined cases (3I3I) was defined as an equivalent amount of 3.43 vertical FRP strips according with the procedure presented in [4].

Finally, the equivalent mechanical effective dynamic stiffness of each case, $E_m I_s$ (see Table 4 and Table 5), was used to analytically calculate the expected vibration frequency ($\omega_{s,calc}$) using (Eq. 2). This calculated value was finally compared with the experimentally obtained one from the modal testing of strengthened walls (ω_s).

3.2. Analytical results

Analytical results are summarised in Table 4 for the first bending vibration shape observed, mode 2, and in Table 5 for mode 4. The effective dynamic elastic stiffness of unstrengthened masonry ($E_m I_u$) is shown in the second column. Third and fourth columns show the effective dynamic stiffness of strengthened walls assuming the static elastic modulus of FRP (170GPa), $E_m I_s^S$, and the dynamic elastic modulus of FRP (204GPa), $E_m I_s^d$, respectively. This dynamic elastic modulus of FRP was calculated from the static one using the relationship obtained by Al-Zubaidy et al. [27] on similar carbon fibre FRP. Fifth and sixth columns gather the values of the calculated vibration frequencies for FRP-strengthened walls in the case of assuming the static ($\omega_{s,calc}^S$) and dynamic ($\omega_{s,calc}^d$) elastic modulus of FRP respectively. Experimental vibration frequency of strengthened

walls is shown in seventh column (ω_s). Finally, the relative errors corresponding to both hypothesis of elastic modulus of FRP are presented in the last two columns (e^s and e^d).

Only the cases with experimental data on modes 2 and 4 for unstrengthened walls are included in result tables (Table 4 and Table 5).

Wall		$E_m I_u$ (Nm ²)	$E_m I_s^s$ (Nm ²)	$E_m I_s^d$ (Nm ²)	$\omega_{s,calc}^s$ (Hz)	$\omega_{s,calc}^d$ (Hz)	ω_s (Hz)	e^s (%)	e^d (%)
2V0H	1	737977	863637	887108	95.6	96.8	97.6	-2.1	-0.8
	2	593080	715971	738577	84.7	86.0	85.1	-0.5	1.1
	3	770326	895535	918996	96.9	98.2	104.8	-7.5	-6.3
3V0H	1	635417	816169	848357	91.6	93.4	90.0	1.8	3.8
	2	722974	905524	938474	96.3	98.1	104.6	-7.9	-6.3
	3	713058	895398	928266	94.4	96.1	95.5	-1.2	0.6
2V2H	1	684527	808908	832031	93.2	94.6	89.5	4.2	5.7
3V5H	1	625505	799380	830430	94.6	96.4	102.1	-7.3	-5.6
	2	731457	909991	942332	100.1	101.8	102.7	-2.5	-0.8
	3	676482	853352	885158	100.5	102.3	103.9	-3.3	-1.5
3I3I	1	572238	768004	802017	87.3	89.2	103.6	-15.7	-13.9
	2	582762	779758	814045	87.9	89.8	100.0	-12.1	-10.2

Table 4. Analytical results for mode 2 shape

Wall		$E_m I_u$ (Nm ²)	$E_m I_s^s$ (Nm ²)	$E_m I_s^d$ (Nm ²)	$\omega_{s,calc}^s$ (Hz)	$\omega_{s,calc}^d$ (Hz)	ω_s (Hz)	e^s (%)	e^d (%)
2V0H	2	1318197	1445846	1470412	339,6	342,5	355,2	-4,4	-3,6
3V0H	1	1627649	1819269	1855836	386,0	389,9	394,6	-2,2	-1,2
2V2H	1	1486914	1615416	1640249	371,8	374,6	378,4	-1,7	-1,0
	2	1160828	1285054	1308864	331,2	334,3	337,9	-2,0	-1,1
	3	1164032	1288844	1312763	331,6	334,7	354,0	-6,3	-5,4
3V5H	1	1359867	1542715	1577373	370,7	374,9	---	---	---
3I3I	1	1374901	1584344	1623754	353,7	358,1	---	---	---

Table 5. Analytical results for mode 4 shape

4. Discussion

First, it has to be highlighted that the only modal shape which was identified in all experimental processes was mode 1, which corresponded to the torsional shape along vertical axis (see images in Table 2). This vibration mode is always associated with the lower vibration frequency. On the other side, mode 4 was only observed in approximately 47% of unstrengthened walls and 30% of FRP-strengthened ones.

In addition, it has to be noticed that all unstrengthened walls were analogous, so their results should be comparable. In this line, the coefficient of variation (CoV) of vibration frequency and damping was calculated for each vibration mode including all walls as a single group. Results, which are shown in the last line of Table 2, indicated that vibration frequency had less variability than damping ratio for all cases except for vibration mode 2, which, in fact, had the lower coefficient of variation in frequency and damping. Hence, vibration frequency is more reliable than damping ratio as comparison parameter to analyse the influence of strengthening installation.

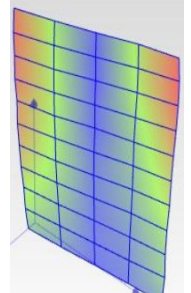
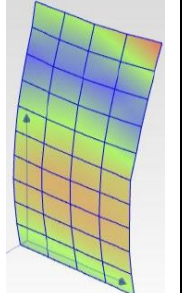
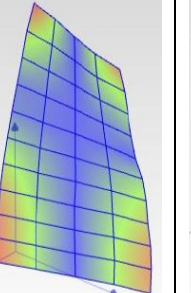
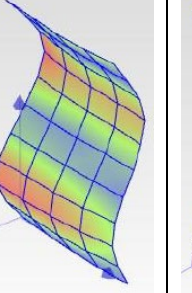
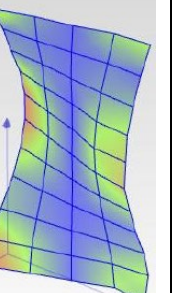
Taking into account this variability on the obtained results, two main ideas arise: i) to properly analyse the effect of strengthening brick masonry walls on their vibrational properties, it is necessary to compare each wall with itself. It is due to the great influence of boundary conditions, geometry differences or particular changes due to manual production of masonry. ii) vibration mode 2, which corresponds to the first observed bending mode of the wall (see image in Table 2), was the less variable one due to masonry heterogeneity and particular boundary conditions.

Experimental results of unstrengthened walls 2V0H-3, 2V2H-3, 3V5H-1 and 3V5H-2 are divergent from the rest of the walls, especially for mode 1 properties. This may be associated to irregular boundary conditions (base support) or to a hypothetical misconnection of some units (partial joints damage). However, taking into account that the strengthened walls did not show this

variability and these were not moved during strengthening operations, the hypothetical irregular base support could be discarded. Hence, it seems that FRP strengthening contributes to uniform the dynamic response of masonry elements minimizing possible manufacturing irregularities or little damages. Nevertheless, this point requires more research to be validated.

Regarding damping ratio analysis, it was noticed that FRP-strengthened walls showed lower damping than the corresponding control walls. Thus, strengthening brick masonry walls with FRP laminates contributes to reduce their vibration damping. It may be related with the stiffness increase associated with FRP strengthening. However, the dispersion of the experimental values of the damping ratio does not allow further quantitative analysis.

Analysing the variation of vibration frequencies (see Table 6) due to FRP-strengthening installation, it was observed that the vibration modes associated with lower frequencies were more reliable (bring results in more cases) than the ones associated with higher frequencies. However, the increase of the vibration frequency was clearly divergent in six particular cases (shadowed in Table 6), which were discarded from the following analyses. None of these cases was related to selected vibration mode 2. All these particular cases corresponded to walls that showed a significantly lower vibration frequency in the unstrengthened configuration in comparison with comparable walls.

<i>Vibration mode</i>				
				
Mode 1	Mode 2	Mode 3	Mode 4	Mode 5
$\Delta\omega$ (%)	$\Delta\omega$ (%)	$\Delta\omega$ (%)	$\Delta\omega$ (%)	$\Delta\omega$ (%)

2V0H	1	3.9	10.8	1.7	---	3.0
	2	4.1	7.7	3.3	6.9	4.3
	3	45.8	16.4	30.0	---	15.8
3V0H	1	3.7	10.2	3.6	6.9	4.1
	2	12.8	20.0	---	---	---
	3	3.8	10.3	2.9	---	4.9
2V2H	1	3.0	5.4	3.1	7.2	---
	2	3.1	---	---	8.4	4.9
	3	104.3	---	6.6	13.4	8.0
3V5H	1	180.0	25.9	63.9	---	33.3
	2	27.7	17.1	18.9	---	24.8
	3	20.2	23.1	19.7	---	---
3I3I	1	25.9	33.5	23.0	---	---
	2	21.7	27.7	21.0	---	27.5
	3	16.7	---	19.1	---	21.4

Table 6. Variation of the vibration frequency of each mode due to the strengthening installation

In order to compare the effect of each strengthening configuration on the variation of the vibration frequencies associated with each vibration mode, results from Table 6 were averaged and these average values are summarised in Figure 4. There, it is observed that out-of-plane bending strengthening (only vertical FRP strips, cases *2V0H* and *3V0H*) was especially detected by the variation of the vibration frequency of mode 2, which reached values over 10% of variation. This result is consistent with the fact that this vibration shape corresponds to an out-of-plane bending deformation on which *2V0H* and *3V0H* strengthening configurations should be more effective because of the alignment of strengthening fibres.

Regarding the effect of orthogonally crossed strengthening configurations (*2V2H* and *3V5H*) on vibration frequencies, similar variations were reported for almost all modes that brought results. However, the particular influence of *3V5H* strengthening on the frequency of the composed mode 5 has to be highlighted because it showed that transversal strips really influenced its overall vibrational response, causing a vibration frequency increase over 15% for all modes and close to 30% for mode 5, which was proved as the more sensitive one for this case. In general terms, the

composed mode 5 was more sensitive for cases with crossed FRP (*2V2H* and *3V5H*) than for the analogous cases without the horizontal strips (*2V0H* and *3V0H* respectively).

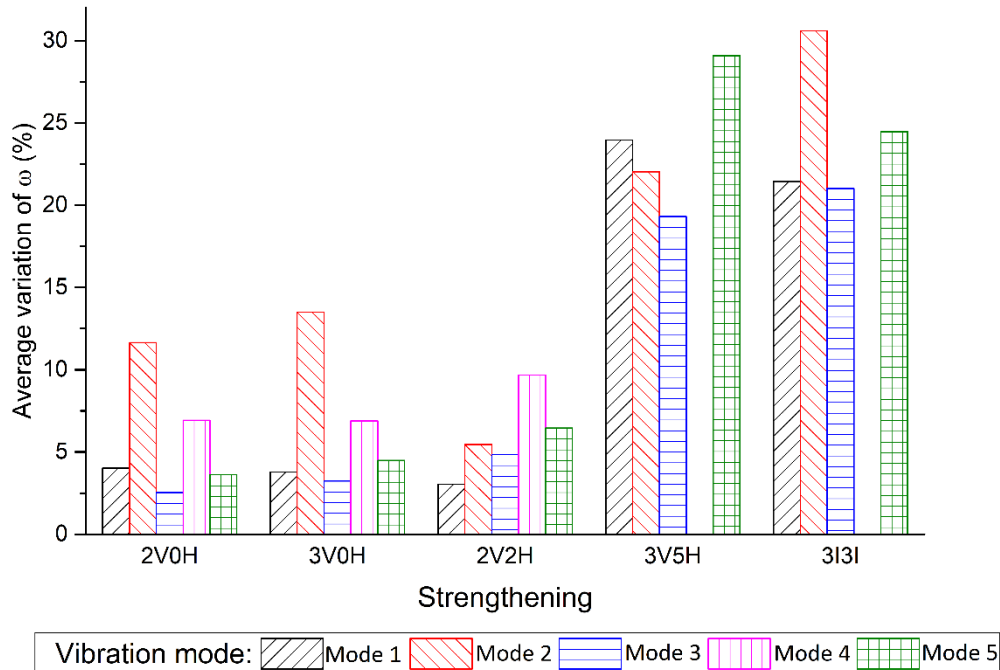


Figure 4. Average of the variation of the vibration frequency for each strengthening type and analysed vibration mode

Like for *3V5H* strengthening configuration, *3I3I* strengthening also increased the vibration frequency of all modes with comparable results. However, in this case, mode 2 was the most sensitive one (average frequency increase over 30%) because of the greater equivalent amount of FRP strips oriented to resist out-of-plane longitudinal bending response of the wall. In fact, the equivalent number of vertical laminates was estimated to 3.43 in [4].

In addition, walls with more strengthening material installed (*3V5H* and *3I3I*) showed greater variation of the values of the vibration frequencies. All comparable vibration modes showed a frequency increase close or over 20% for *3V5H* and *3I3I* cases, whereas it was lower than 15% for

all other strengthening configurations. Hence, increasing the strengthening amount is related with a stiffness increase of the strengthened structure.

This relationship between strengthening amount and variation of the vibration frequency is also supported by the comparison between *2VOH* and *3VOH* cases, which showed a frequency increase of mode 2 of 11.6% and 13.5% respectively. In addition, analytical calculations also pointed out this effect: bonding a stiffer material (FRP laminate) increases the stiffness of the wall and it causes an increase of the vibration frequency according with (Eq. 1). Experimentally, all strengthened cases showed increased vibration frequencies in comparison with their un-strengthened configuration. In the same line, the stiffer response of strengthened walls and the relationship between strengthening amount and equivalent wall stiffness was also presented as a result of the corresponding destructive tests under eccentric axial load of the analysed walls (see[4]).

However, mode 4 was not detected for any case with *3V5H* or *3I3I* strengthening configurations. It is a non-expected result because this bending mode 4 was supposed to be really influenced by these strengthening configurations. It is suspected that it may be due to the increase of the associated vibration frequency over the threshold limit defined in the data acquisition (500Hz) although more research would be necessary in this line to validate this statement.

To finish with the analysis of the experimental results, it is observed that mode 2 is the most sensitive one if comparing tested cases altogether.

In Table 4 and Table 5 it is observed that the vibration frequency associated to the bending modal shapes (mode 2 and mode 4) can be predicted for strengthened elements using vibration information of the unstrengthened structure and the properties of the strengthening materials.

For both vibration modes, the relative error of the predicted vibration frequency was always below 10% except for the cases *3I3I* regarding mode 2. This particular higher error may be due to

an out of order low value of the vibration frequency of walls 3I3I_1 and 3I3I_2 before strengthening them (8.5% lower than the rest of results for mode 2).

The average of the absolute values of relative errors (not taking into account cases 3I3I) were 3.8% and 3.3% for the comparison of experimental results of vibration frequencies of mode 2 and predicted values using static and dynamic elastic modulus of FRP respectively. Similarly, errors of 3.3% and 2.5% were respectively obtained for the cases of using static and dynamic elastic modulus of FRP for the mode 4. Thus, it is observed that predictions that used dynamic elastic modulus of FRP achieved more accurate results than the ones that used static elastic modulus of FRP. Nevertheless, this difference is little. In addition, analytical results using static elastic modulus of FRP were conservative, so predicted frequencies tended to be lower than experimentally observed ones (see Table 4 and Table 5). Hence, it would be recommended to use the proposed analytical methodology and the static value of the elastic modulus of FRP to calculate the minimum expected vibration frequency associated to a pure bending modal shape of an FRP strengthened masonry element.

Finally, the agreement between the results of the analytical calculation and the experimental values of vibration frequencies (see relative errors in Table 4 and Table 5) supports the idea that modal analysis can be a useful tool to assess the structural performance of FRP strengthening interventions. Hence, it is possible to assess the vibrational parameters of an original structure (unstrengthened) and use those data to calculate the expected vibration frequencies after strengthening. When strengthening installation is performed, a new modal analysis should be carried out to check if the expected variation of the frequencies associated with pure bending modal shapes has been achieved. This comparison would define a quality criterion of the strengthening action.

4.1. Discussion on the extension to practical cases

Although the applied methodology proves to be efficient at determining changes on the vibrational response of stand-alone brick masonry walls due to strengthening with FRP laminates, further reflexions need to be considered before extending the in-lab proposed method to real buildings.

First of all, the particular methodology which was implemented (input-output experimental modal identification tests) is useful for little structures but it would be required to turn into operational modal analysis (ambient modal identification) if the aim is determining the influence of a strengthening intervention on a whole building, bridge, etc. The adaptation to operational modal analysis is out of the scope of the current research and it requires further tests on bigger structures using an extensive distribution of accelerometers. Nevertheless, input-output experimental modal identification tests will remain useful to analyse the influence of punctual strengthening interventions on structurally well-defined (including their boundary conditions) elements, like simply supported concrete beams.

In addition, it is well-known that the applied load can influence of the vibrational response of a structure. Hence, the pre-strengthening and post-strengthening modal analysis should be carried out with equivalent applied loads to obtain comparable results and being able to discuss about the effectiveness of the strengthening intervention. The influence of varying applied loads on vibrational response should also be investigated in future campaigns to extend the results presented in this manuscript.

Regarding the boundary conditions and possible openings on the walls, it is clear that all those parameters influence on the vibrational response of a wall which is part of a real building. In general terms, it has to be taken into account that the stiffer boundary conditions or geometric

definitions, the little influence it is expected to be detected by the proposed methodology. However, further experimental researches need to be carried out to check this common sense general intuition and set the threshold applicability point of the proposed method.

Finally, the possibility of applying the developed methodology on damaged structures, different masonry materials or different masonry elements (e.g. arches, vaults) is supported by previous researches found in the literature review ([21,24]) which used modal analysis to characterise them. In addition, experimental tests that can be generally found in literature show that the stiffness on any structure is modified when a stiffer strengthening (like FRP, which is stiffer than most of the general building materials) is applied. This effect is expected to be greater for damaged structures, enhancing the applicability of the proposed method in this case because of the little stiffness of damaged structures. Similarly, dry masonry or stone masonry with low stiffness mortars are also expected to be very sensitive to changes in vibrational response when FRP strengthening is applied because of their initial lower stiffness. Nevertheless, it has to be also recognised that the particular influence of punctual little strengthening interventions (for example a single wall of a whole building) would hardly modify the general vibration parameters of complex large buildings. In this case, input-output experimental modal identification tests may be used to determine the vibrational response of the strengthened element only, leaving the rest of the building to simply contribute to: (i) the particular boundary conditions and (ii) additional vibrational response that had to be eliminated from the analysis by comparing pre-strengthened and post-strengthened response of the punctual strengthened structural element.

5. Conclusions

The general and application focused conclusions that arise from the presented research are:

- Experimental Modal analysis is a suitable tool to assess the performance of FRP-strengthening interventions on structural masonry elements.
- The effect of FRP-strengthening of punctual elements of a building is not expected to be detected by the vibrational analysis of the full building. In addition, this global analysis should use operational modal analysis techniques which are not assessed in the current research.
- Evidences support the use of the proposed method for different types of masonry, different structural elements or different boundary conditions or loading cases with the only restriction that the pre- and post-strengthening conditions should remain the same.
- Evidences support that the proposed method is more effective on structures with little initial stiffness because the stiffness change due to the FRP-strengthening is relatively more significant.

After performing modal testing on fifteen brick masonry walls before and after strengthening them with FRP strips installed with five different configurations, the particular conclusions are:

- Vibration modes associated with lower frequencies (<90Hz) are easier to be observed than modes associated with higher frequencies. In fact, vibration mode 1 is the only one observed for all (strengthened and unstrengthened) cases.
- Vibration frequency is more suitable than damping ratio as comparison parameter for assessing the effect of FRP strengthening because of its lower coefficient of variation.
- FRP strengthening reduces damping ratio.
- The FRP-strengthening pattern determines the vibration modes which are mode affected by its installation.

- Increasing the amount of the FRP installed causes an increase of the variation of the vibration frequencies. (Eq. 1) can be used to calculate this relationship for pure bending modes.
- Mode 2 is the most reliable one to perform the assessment on the strengthening effectiveness for the considered walls because it is the most sensitive mode to the frequency vibration changes associated with FRP installation and it is the one with less variability for the unstrengthened walls. The most suitable vibration mode can change for different structures, boundary and loading conditions.

In addition, taking into account the analytical results it can be concluded that:

- It is necessary to base analytical calculations of the vibration frequencies of strengthened structures on experimental results of the same structures before strengthening.
- The definition of a homogenised equivalent section allows taking into account FRP strengthening of masonry walls for analytical calculation purposes.
- The theoretical variation of vibration frequencies, which is analytically calculated, is precisely observed (error below 5%) in experimental modal analysis results for pure bending modes.
- The proposed analytical methodology is more accurate when the dynamic elastic modulus of the strengthening material is used instead of the static one.

Acknowledgements

First author is a Serra Hünter Fellow. Authors want to acknowledge the contribution of SAHC's Master student Hamid Reza Taravat on developing experimental tests.

Funding

This work was supported by MULTIMAS research project (BIA2015-63882-P) by the Spanish Government.

References

- [1] Minafò G, Monaco A, D'Anna J, La Mendola L. Compressive behaviour of eccentrically loaded slender masonry columns confined by FRP. *Eng Struct* 2018;172:214–27. doi:10.1016/j.engstruct.2018.06.011.
- [2] Witzany J, Čejka T, Zigler R. Failure mechanism of compressed short brick masonry columns confined with FRP strips. *Constr Build Mater* 2014;63:180–8. doi:10.1016/j.conbuildmat.2014.04.041.
- [3] Santa-Maria H, Alcaïno P. Repair of in-plane shear damaged masonry walls with external FRP. *Constr Build Mater* 2011;25:1172–80. doi:10.1016/j.conbuildmat.2010.09.030.
- [4] Bernat-Maso E, Gil L, Escrig C. Analysis of brick masonry walls strengthened with fibre reinforced polymers and subjected to eccentric compressive loads. *Constr Build Mater* 2015;84. doi:10.1016/j.conbuildmat.2015.02.078.
- [5] Lorenzis L De, Ochsendorf J. Failure of rectangular masonry buttresses under concentrated loading. *Proc ICE - Struct Build* 2008;161:265–75. doi:10.1680/stbu.2008.161.5.265.
- [6] Mahini SS, Eslami a., Ronagh HR. Lateral performance and load carrying capacity of an unreinforced, CFRP-retrofitted historical masonry vault – A case study. *Constr Build Mater* 2012;28:146–56. doi:10.1016/j.conbuildmat.2011.08.013.
- [7] Fossetti M, Minafò G. Comparative experimental analysis on the compressive behaviour of masonry columns strengthened by FRP, BFRCM or steel wires. *Compos Part B Eng* 2017;112:112–24. doi:10.1016/j.compositesb.2016.12.048.
- [8] Marcari G, Manfredi G, Prota A, Pecce M. In-plane shear performance of masonry panels strengthened with FRP. *Compos Part B Eng* 2007;38:887–901. doi:10.1016/j.compositesb.2006.11.004.
- [9] Batikha M, Alkam F. The effect of mechanical properties of masonry on the behavior of FRP-strengthened masonry-infilled RC frame under cyclic load. *Compos Struct* 2015;134:513–22. doi:10.1016/j.compstruct.2015.08.105.
- [10] Gattesco N, Boem I. Out-of-plane behavior of reinforced masonry walls: Experimental and numerical study. *Compos Part B Eng* 2017;128:39–52. doi:10.1016/j.compositesb.2017.07.006.
- [11] Willis CR. Design of unreinforced masonry walls for out-of-plane loading. University of

Adelaide, 2004.

- [12] Alotaibi KS, Galal K. Axial compressive behavior of grouted concrete block masonry columns confined by CFRP jackets. *Compos Part B Eng* 2017;114:467–79. doi:10.1016/j.compositesb.2017.01.043.
- [13] Hamed E, Rabinovitch O. Lateral out-of-plane strengthening of masonry walls with composite materials. *J Compos Constr* 2010;14:376.
- [14] Luccioni B, Rougier VC. In-plane retrofitting of masonry panels with fibre reinforced composite materials. *Constr Build Mater* 2011;25:1772–88. doi:10.1016/j.conbuildmat.2010.11.088.
- [15] Cancelliere I, Imbimbo M, Sacco E. Experimental tests and numerical modeling of reinforced masonry arches. *Eng Struct* 2010;32:776–92. doi:10.1016/j.engstruct.2009.12.005.
- [16] Maljaee H, Ghiassi B, Lourenço PB, Oliveira D V. Moisture-induced degradation of interfacial bond in FRP-strengthened masonry. *Compos Part B Eng* 2016;87:47–58. doi:10.1016/j.compositesb.2015.10.022.
- [17] ACI Committee 440. ACI 440.7R-10 Guide for the Design and Construction of Externally Bonded Fiber-Reinforced Polymer Systems for Strengthening Unreinforced Masonry Structures. Farmington Hills: American Concrete Institute; 2010.
- [18] Dong Y, Ansari F. 7 - Non-destructive testing and evaluation (NDT/NDE) of civil structures rehabilitated using fiber reinforced polymer (FRP) composites. In: Karbhari VM, Lee LS, editors. *Serv. Life Estim. Ext. Civ. Eng. Struct.*, Woodhead Publishing; 2011, p. 193–222. doi:https://doi.org/10.1533/9780857090928.2.193.
- [19] Lorenzoni F, Valluzzi MR, Salvalaggio M, Minello A, Modena C. Operational modal analysis for the characterization of ancient water towers in Pompeii. *Procedia Eng* 2017;199:3374–9. doi:10.1016/j.proeng.2017.09.446.
- [20] Torres W, Almazán JL, Sandoval C, Boroschek R. Operational modal analysis and FE model updating of the Metropolitan Cathedral of Santiago, Chile. *Eng Struct* 2017;143:169–88. doi:10.1016/j.engstruct.2017.04.008.
- [21] Prado DM, Araujo IDG, Haach VG, Carrazedo R. Assessment of shear damaged and NSM CFRP retrofitted reinforced concrete beams based on modal analysis. *Eng Struct* 2016;129:54–66. doi:10.1016/j.engstruct.2016.09.058.
- [22] Bernat-Maso E, Teneva E, Escrig C, Gil L. Ultrasound transmission method to assess raw earthen materials. *Constr Build Mater* 2017;156:555–64. doi:10.1016/j.conbuildmat.2017.09.012.
- [23] Corradi M, Borri A, Castori G, Coventry K. Experimental analysis of dynamic effects of FRP reinforced masonry vaults. *Materials (Basel)* 2015;8:8059–71. doi:10.3390/ma8125445.
- [24] Cakir F, Uysal H. Experimental modal analysis of brick masonry arches strengthened prepreg composites. *J Cult Herit* 2015;16:284–92. doi:10.1016/j.culher.2014.06.003.

- [25] Bernat E, Gil L, Roca P, Sandoval C. Experimental and numerical analysis of bending–buckling mixed failure of brickwork walls. *Constr Build Mater* 2013;43:1–13. doi:<http://dx.doi.org/10.1016/j.conbuildmat.2013.01.025>.
- [26] Tirelli D. Modal Analysis of Small & Medium Structures by Fast Impact Hammer Testing Method. 2011. doi:10.2788/80576.
- [27] AL-Zubaidy H, Zhao XL, Al-Mihaidi R. Mechanical behaviour of normal modulus carbon fibre reinforced polymer (CFRP) and epoxy under impact tensile loads. *Procedia Eng* 2011;10:2453–8. doi:10.1016/j.proeng.2011.04.404.